Available online at www.sciencedirect.com
SCIENCE DIRECT®
Physica C 384 (2003) 1–10
PHYSICA C
www.elsevier.com/locate/physc

Electronic transport in MgB_2, AlB_2 and ZrB_2—a comparative study

B. Fisher *, K.B. Chashka, L. Patlagan, G.M. Reisner

Physics Department and Crown Center for Superconductivity, Technion, Haifa 32000, Israel

Received 24 July 2002; received in revised form 1 October 2002

Abstract

We report on the temperature dependence of the resistivity (ρ) and the absolute thermopower (S) of the polycrystalline title materials and of AlB_2 single crystals. For all samples $\rho(T)$ exhibits a Bloch–Grüneisen-like temperature dependence, with large characteristic temperatures θ_R ($\approx\theta_D$—the Debye temperature). At high temperatures the thermopower $S(T)$ for ZrB_2 (n-type) is almost the mirror image of $S(T)$ for MgB_2 (p-type) while $S(AlB_2)$ is very small for all temperatures. The density of states distribution $N(E)$ around E_F seems to play a dominant role in determining $S(T)$ of these materials. $\ln(T)$ terms in the low-temperature $\rho(T)$ and $S(T)$ of ZrB_2 samples bear evidence for weak localization in 2D.

PACS: 74.70.Ad; 72.15.Jf; 72.15.Rn; 71.20.Gj
Keywords: Superconductivity; Thermopower; Weak localization; Density of states

1. Introduction

Since the discovery of superconductivity in MgB_2 [1], many studies of its normal state transport properties have been carried out. Experimental results [2–7] show that its resistivity $\rho(T)$ exhibits a Bloch–Grüneisen-like (BG) temperature dependence typical for phonon scattering in a simple metal with a high Debye temperature, superimposed on a constant (residual) resistivity ρ_0. The textbook BG formula is [8,9]:

$$\Delta\rho(T) = \rho - \rho_0 = A\left(\frac{T}{\theta_R}\right)^5 J_5(\theta_R/T) \tag{1}$$

where ρ_0 is the residual resistivity, A is a constant and θ_R is a characteristic temperature, usually close to θ_D—the Debye temperature deduced from specific heat; $J_5 = \int_0^x z^5\,dz/[(e^z-1)(1-e^{-z})]$ where $x = T/\theta_R$. In a generalized BG formula (BG(n)) the power 5 and J_5 are replaced by n and J_n. At low temperatures $\Delta\rho(T) \propto T^n$. For high quality MgB_2 samples (with low ρ_0) n is closer to 3 [3–7]. Therefore, in Refs. [3–5] the BG(3) formula was fitted to the experimental $\rho(T)$. $\Delta\rho(T)$ expressed by the BG(3) formula may be associated with interband electron–phonon scattering [10]. The fitted θ_R values for BG(3) are higher than those for BG(5) and also larger than most θ_D values obtained from heat capacity measurements.

* Corresponding author. Tel.: +972-4-8293652; fax: +972-4-8221514.
E-mail address: phr06bf@physics.technion.ac.il (B. Fisher).

0921-4534/02/$ - see front matter
PII: S0921-4534(02)02280-3

A number of studies were devoted to the thermopower of MgB_2 [4,11–15]. The absolute thermopower (S) of MgB_2 is positive for all temperatures above T_c and increases quasilinearly with T in the range $40 \leqslant T \leqslant 150$ K; the extrapolated value of S at $T = 0$ has a small but finite negative value and above $\sim$150 K S becomes nonlinear and exhibits a tendency towards saturation. The quasilinear $S(T)$ was analyzed in terms of diffusion thermopower (S_D) dominated by holes; the negative intercept of S at $T = 0$ was attributed to phonon drag [11,15] and the deviation from linearity at high temperature to electron-like states adding a negative contribution at high temperatures. In the earlier publications the linear portion of $S(T)$ was interpreted in terms of Mott's formula for diffusion thermopower of a degenerate electron gas [8,9]:

$$S_D = -\frac{\pi^2 k_B^2 T}{3|e|}\left[\frac{\partial \ln \sigma(E)}{\partial E}\right]_{E=E_F} = -\frac{\pi^2}{3}\frac{k_B^2 T}{|e|E_F}\xi \quad (2)$$

where $\sigma(E)$, would be the conductivity measured for E_F at E, $\xi = [\partial \ln(\sigma(E))/\partial \ln E]_{E_F}$ and E_F is measured from the band edge. For spherical Fermi surfaces $\xi = 1$ for scattering by impurities (constant mean-free-path) and $=3$ for quasi-elastic phonon scattering [8,9]. For holes, the corresponding values of ξ are negative. In metals with more complicated Fermi surfaces ξ deviates strongly from these ideal values and its sign may be unrelated to the type of the carriers. [1] The Fermi energy of carriers in MgB_2, estimated [11] by fitting Mott's formula with $\xi = -1$ to the linear portion of $S(T)$ was found in fair agreement with that obtained from band structure calculations. Good agreement between the fitted E_F and band calculation is claimed also in Ref. [15], although different parameters were employed in the latter interpretation. MgB_2 is a multi-band system [16–19] with complicated Fermi surfaces. In Ref. [4] the Seebeck tensor S_D was calculated using the two pairs of bands (σ and π) that contribute to the conductivity of MgB_2. The general expressions for the tensor's components were calculated instead of using Mott's approximation; an isotropic relaxation time, independent on energy, was assumed in that work and a strong phonon drag contribution was included. The calculated $S(T)$, representing an average over all directions is in semiquantitative agreement with the experimental $S(T)$ and reproduces the main features of the dependence on temperature and on Al-doping. This shows that in undoped MgB_2 the contribution of the σ bands to S exceeds by far that of the π bands. $S(T)$ in MgB_2 may be regarded as fairly simple in spite of the material's complex electronic structure and complications mentioned below:

- The scattering mechanisms dominating transport in each of the bands of MgB_2 are presently under debate [18,20–22]. The role of the electron–phonon interaction in the thermopower of metals at $T < \theta_D$, is not trivial and has been the subject of many studies that did not yet lead to a consensus [23,24]. MgB_2 (and many other diborides) have very high Debye temperatures, typically between 500 and 1000 K [25], thus the interesting regime for their thermopower is $T < \theta_D$ where the phonon scattering is inelastic.
- All measurements reported so far have been carried out on polycrystalline samples. In such samples it is difficult to distinguish between the contributions of impurity scattering in the bulk and grain-boundary resistance to the residual resistivity (thermopower is insensitive to grain-boundaries). Moreover, a material formed of anisotropic, randomly oriented crystallites appears as if it is multiphase. The thermopower of such a system may be affected by the anisotropy of ρ, of the heat conductivity and of S [26].

The solution of the theoretical problems as well as the growth of MgB_2 single crystals (SCs) (with controlled impurity content) may take some time. At this stage, it was interesting to find out if the relative simplicity of $S(T)$ for MgB_2 is accidental or if it is common among the diborides. In particular we looked for a correlation between the density of states (DOS) distribution function $N(E)$ which is known for many diborides and $S(T)$. For spherical equi-energy surfaces and elastic scatter-

[1] Even the sign of S for Cu, Ag and Au (which are simpler than MgB_2 in all respects) was not understood for many decades.

ing this correlation is straightforward, but for real metals, even elemental and monovalent, it is not.

Except for MgB_2, all known diborides of hexagonal structure are either non-superconducting or low-T_c superconductors [27]. Although many have been investigated in the past, we found in the literature detailed results of $S(T)$ only for TiB_2 [28]. It is more complicated than $S(T)$ for MgB_2, exhibiting a sign change from p-type at low-T, to n-type at high-T, and rather poor reproducibility from sample to sample. E_F of TiB_2 lies at a minimum of the DOS, in a "pseudogap" [25,29]. Our choices of diborides for electronic transport measurements were AlB_2 and ZrB_2. Following Mg which is divalent, Al is trivalent and Zr—tetravalent. As summarized below, these materials are interesting for additional reasons.

Thirty years ago it has been pointed out that although AlB_2 is the prototype structure for many diborides, nothing has been reported on its electrical properties [30]. Room temperature (RT) resistivity and Hall effect measurements were reported in that work; the RT Hall constants of several samples were p-type and consistent with $p \leqslant 1$ hole/unit cell. It seems that since then not much has been published on this topic. X-ray spectroscopy results published before [31] and after [32,33] the discovery of superconductivity in MgB_2 show that as in the case of TiB_2, E_F of AlB_2 lies in a pseudogap. This is in contrast with the large DOS at E_F in MgB_2. Polarization-dependent X-ray emission and absorption in SCs of AlB_2 showed that E_F lies well above the σ band. Al can substitute Mg to form $Mg_{1-x}Al_xB_2$ in a wide range of concentrations [34]. This substitution leads first to a decrease in T_c and then to the disappearance of superconductivity, consistent with expectations from electronic structure calculations [16]. For low values of x the thermopower increases with x [11]; this is consistent with the shift of E_F towards the σ band-edge.

ZrB_2 is remarkable: it is a hard, refractory material, its melting point ($\sim$3000 °C) is much higher than that of its constituents, and it is a very good conductor although its electronic structure is not that of a metal [35]. The Hall constants obtained in the sixties were consistent with a very low, temperature independent electron concentration [36]. Early [35,37] and recent band structure calculations [38–40] show that its E_F lies in a "pseudogap"; close inspection of the figures of Refs. [35,38–40], reveals that E_F lies slightly above the dip, that is, where $dN(E)/dE > 0$. Superconductivity at 5.5 K was recently reported for a sintered ZrB_2 sample [41] but it was later attributed to a minority phase [42]. According to Ref. [39], the low value of $N(E_F)$ and the weak electron–phonon coupling (obtained from specific-heat measurements) seem inconsistent with $T_c =$ 5.5 K. In our investigation we found marks of superconductivity in a porous ZrB_2 sample sintered at low temperature. The resistivity and thermopower of samples sintered at high temperatures exhibit logarithmic temperature dependencies, typical for weak localization in 2D.

We tried to grow crystals of all three materials; so far only some of our AlB_2 SCs have reasonable dimensions for resistivity and thermopower measurements. It will be shown however that the thermopower of polycrystalline AlB_2 is close to that of AlB_2 SCs. The results for our MgB_2 samples agree with the earlier results and confirm the weak sensitivity of its $S(T)$ to microstructure. The apparent systematics of $S(T)$ as function of valence is one of the significant findings of this work: while the $S(T)$ graphs for ZrB_2 samples (n-type) are almost mirror images of those for MgB_2 samples (p-type), $S(AlB_2)$ is very low at all temperatures.

2. Experimental

2.1. Sample preparation and characterization

MgB_2. Polycrystalline MgB_2 was prepared via various protocols. Here we report on two very different types of MgB_2: (a) non-annealed (NA)—formed by RT compression of Alpha-Aesar MgB_2 powder and (b) hot pressed (HP)—annealed for several hours at 1000 °C under a pressure of 20 MPa. [2]

[2] The hot-pressed annealing of MgB_2 and sintering of ZrB_2 at high temperatures has been carried out at the Ceramic and Silicate Institute, Technion City.

ZrB_2. One set of samples was prepared by the standard solid state synthesis from the elements in stoichiometric ratio. The bar-shaped samples were annealed twice at 1500 °C in flowing Ar5%H_2 with intermediate grinding. They were very porous and brittle but on one of them (sample S1) we were able to carry out transport measurements. Rigid samples were obtained by sintering of pressed powder at 1800 °C in Ar atmosphere for 1 h. [2] The raw materials for the high temperature sintering were (a) the powder prepared before from the elements (sample S2) and (b) commercial (Art) ZrB_2 powder with a small boron deficiency (of 0.23% of the total mass) and carbon and oxygen impurities (0.6% and 1.4% of the total mass, respectively). We attempted to grow SCs by slow cooling of molten aluminum solutions of ZrB_2 [43]. The dominant products of two such attempts were mm size rectangular platelets later identified via X-ray diffraction (XRD) as Al_3Zr SCs. A minority of sub-mm size hexagonal crystallites were later identified as ZrB_2, however these were too small for transport measurements.

AlB_2. Sub-mm up to mm size, ~10 μm thick SCs were grown by slow cooling of molten aluminum solutions, following a protocol similar to those of Refs. [30,33]. Slightly larger and thicker (20–40 μm thick) crystals were obtained (unintentionally) as a by-product of hexaborides' SC growth [44]. It is easier to grow SCs of AlB_2 from molten aluminum solution than to sinter pellets of high purity powder. This is due to the decomposition of AlB_2 into AlB_{12} + Al in the absence of excess Al [45]. Here we report on a NA, polycrystalline sample—formed by RT compression of AlB_2 powder (Aldrich 99%); it was relatively rigid and robust.

The XRD patterns for all polycrystalline samples show no foreign phases except for traces of MgO in the HP MgB_2 samples and of ZrO_2 in ZrB_2 S1. The diffraction pattern of the ZrB_2 samples grown at 1800 °C showed no traces of impurities.

2.2. Resistivity, thermopower and AC susceptibility measurements

The resistivity of bar-shaped samples was measured by the standard four-probe method in a closed cycle refrigerator or on a cold finger of a He cryostat. The thermopower measurements on polycrystalline samples were carried out in a He cryostat from 5 K up to RT. In a separate system, that may be adapted to small and fragile samples and can be heated from liquid N_2 temperature up to 400 K, we measured the thermopower of AlB_2 SCs and of the polycrystalline samples (the latter above RT). The thermal emf was measured between the copper wires of two copper-constantan thermocouples with their junctions embedded in the copper heat sinks bridged by the samples; S was obtained by adding S(Cu) to the measured thermal emf. For some unknown reason, it was very difficult to obtain good thermal contacts to the ZrB_2 samples in the system for high temperature thermopower measurements. Good thermal contacts were obtained once for sample S2 but above 340 K they were lost and the measurements became irreproducible.

AC susceptibility of ZrB_2 was measured in a home-built susceptometer based on Oxford Teslatron, with a frequency of 1 KHz.

3. Experimental results

3.1. Temperature dependence of resistivity

For all samples investigated in this work $\rho(T)$ exhibited a BG-like temperature dependence. We analyzed the experimental traces in terms of the textbook BG formula with $n = 5$ (see Eq. (1)). The fitting parameters ρ_0, A and θ_R for each sample are given in Table 1. We also added the $\rho(RT)/\rho_0$ data. Values of θ_D for MgB_2 and ZrB_2, from the literature, are shown in the last column of Table 1. (No datum was found for AlB_2). The reduced resistivities of all samples $\Delta\rho(T)/\Delta\rho(\theta_R)$ are plotted as function of the reduced temperature T/θ_R, in Fig. 1. All data fall close to the solid line which represents the theoretical BG function. Since for all samples ρ_0 is much larger than $\Delta\rho(T < 100\ K)$ the fit is biased by the high temperature data.

Both MgB_2 HP and NA samples were superconducting with $T_c = 38.3$ and 36 K, respectively in spite of their different resistivities: $\rho_0(NA)/\rho_0(HP) \sim 140$ (!) and $A(NA)/A(HP) = 8$. The

Table 1
Fitting parameters of the BG formula to $\rho(T)$ for various samples of MgB_2, AlB_2 and ZrB_2

Sample	Type	Relative density	$\rho(RT)/\rho_0$	ρ_0 (Ω cm)	A (Ω cm)	θ_R (K)	θ_D (K)
MgB_2 HP	Hot pressed	0.8	3.0	1.12×10^{-5}	4.09×10^{-4}	862 ± 18	750–1050[a]
MgB_2 NA	NA	0.8	1.2	1.54×10^{-3}	3.16×10^{-3}	797 ± 13	
AlB_2 SC1	Single crystal[b]		1.4	1.89×10^{-4}	9.63×10^{-4}	749 ± 14	
AlB_2 SC2	Single crystal [b]		1.4	1.41×10^{-4}	1.11×10^{-3}	956 ± 13	
AlB_2 SC3	Single crystal[c]		1.4	1.35×10^{-4}	6.20×10^{-4}	706 ± 16	
AlB_2 NA	NA	0.65	1.1	2.11×10^{-3}	2.17×10^{-3}	524 ± 20	
ZrB_2 S1	Sintered (1500 °C)	0.55	1.7	6.20×10^{-4}	5.67×10^{-3}	712 ± 16	585, 630[d]
ZrB_2 S2	Sintered (1800 °C)	0.65	3.9	7.71×10^{-6}	2.70×10^{-4}	666 ± 4	
ZrB_2 S3	Sintered (1800 °C)	0.72	2.2	1.05×10^{-5}	1.49×10^{-4}	678 ± 8	

[a] See Refs. [4,48] and references therein.
[b] Obtained unintentionally during growth of CaB_6 following the protocol in Ref. [44].
[c] Obtained following the protocol in Ref. [30].
[d] See Tables 3 and 4 in [25] and references therein.

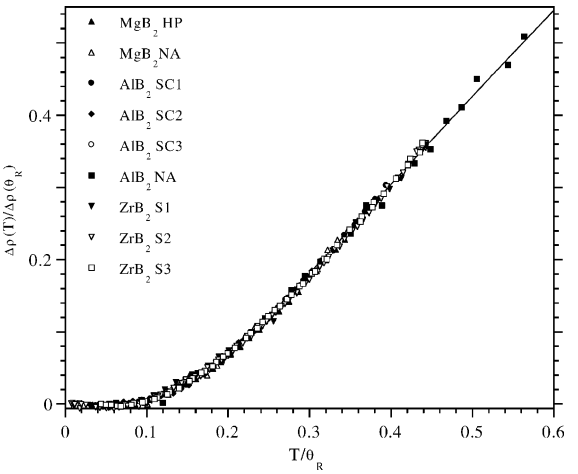

Fig. 1. $\Delta\rho(T)/\Delta\rho(\theta_R)$ versus T/θ_R for various MgB_2, AlB_2 and ZrB_2 samples. The solid line represents BG function (Eq. (1)). The fitting parameters for each sample are shown in Table 1.

large values of ρ_0 indicate that at least for the NA sample the resistivity is dominated by grain-boundaries. The fairly large ratio of $A(NA)/A(HP)$ indicates that a large part of the grain boundaries of the NA sample probably blocks the current. The values of θ_R for these two samples (and of additional samples investigated by us) are close and fall within the range of θ_D values obtained from lattice measurements.

The RT resistivities of our AlB_2 SCs are larger than those cited in Ref. [30] by factors of 3–9. For all three SCs, $\rho(RT)/\rho_0 = 1.4$; their resistivity seems to be dominated by impurity scattering. For the porous, NA sample this ratio is only 1.1. In this case, a large part of ρ_0 is probably due to grain boundaries. The values of the fitted θ_R are spread over a range that is much wider than those for MgB_2 or ZrB_2. This is in spite of the fact that $\rho(RT)/\rho_0$ for the MgB_2 NA and AlB_2 NA samples are comparable and the porosity of the ZrB_2 S1 sample is larger than that of the AlB_2 NA sample. We looked therefore for a process that may compete with electron–phonon scattering leading to a BG type $\rho(T)$. Such a process is the scattering from vibrating impurities. This mechanism known as "electron–phonon–impurity-interference" was analyzed in detail by Reizer and Sergeev [46]. Its signature is the behavior of $\rho(T)$ at temperatures far below θ_D: $\Delta\rho_{Int} = \rho - \rho_0 = \rho_0 BT^2$ where B is a constant. The reduced resistivities $\Delta\rho(T)/\Delta\rho(\theta_R)$ calculated from the BG formulae BG(5) (Eq. (1)) and BG(3), and the Reizer and Sergeev (RS) formula [46] are plotted as function of the reduced temperature T/θ_R, in Fig. 2(a). It can be seen that up to $T \approx 0.1\theta_R$, $\Delta\rho(T) \propto T^5$ and T^3 according to the BG formulae and $\propto T^2$ according to the RS formula; with increasing T the slope drops gradually towards 1 for the first two cases and 0 for the

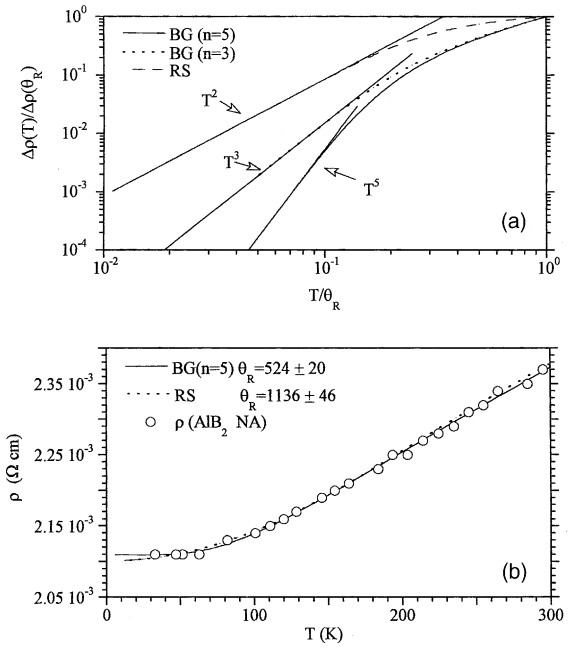

Fig. 2. (a) $\Delta\rho(T)/\Delta\rho(\theta_R)$ versus T/θ_R given by the BG functions with $n = 5$ and 3 and the RS functions, (b) ρ versus T for sample AlB_2 NA, with the BG(5) and RS functions fitted to the plot of the experimental data. Note that the values of θ_R for the fitted BG(5) and RS functions differ by more than a factor of two.

third. Around $T/\theta_D = 1/3$ the BG $(n = 5)\Delta\rho(T) \propto T^2$; if the temperature dependence of the resistivity is minor due to a large ρ_0, and θ_D is unknown, it is hard to distinguish between the BG and RS temperature dependencies (or their combination). The analysis of $\rho(T)$ for the AlB_2 NA sample in terms of the two alternative formulae is a good example for this uncertainty. Fig. 2(b) shows the two lines fitted to the experimental plot. The fitted θ_R value for the RS formula is more than twice larger than that for the BG formula. $\Delta\rho(T < 100$ K) for the three SCs was plotted as function of T^2 and as function of T^5 and linear functions were fitted to the plots. The R^2 of the lines fitted to the $\Delta\rho$ versus T^2 plots were higher but not enough to prove that the low-T resistivity is governed by the RS mechanism. The spread of the θ_R values among the SCs indicates that the two mechanisms probably compete at low temperatures; this implies that $\theta_R(AlB_2)$ is about 1000 K.

ZrB_2 sintered at 1500 °C was very porous and brittle. However it was possible to carry out both resistivity and thermopower measurements on such a sample. Upon increasing the sintering temperature of ZrB_2 from 1500 to 1800 °C, ρ_0 dropped by about two orders of magnitude and A—by more than one. High temperature sintering heals most of the grain boundaries, as hot pressing does in the case of MgB_2. The material sintered at the higher temperature is very rigid although its density is much lower than the ideal density (see relative densities of samples S2 and S3 in Table 1).

The resistivities of ZrB_2 samples S2 and S3 are larger but of the same order of magnitude as that reported in Ref. [41]. $\rho(T)$ of these samples exhibited a shallow minimum around 40 K which is barely resolved from the noise in the case of S2. No drop in $\rho(T)$, that could be associated with transition to superconductivity, was detected in this sample down to $T = 4.75$ K. The clear minimum of $\rho(T)$ of sample S3 seen in Fig. 3 was obtained under very slow cooling. Attempts were made to fit several functions to the regime where the temperature coefficient of resistivity is negative. The best fit to the experimental data for $7 \leqslant T \leqslant 40$ K, and a very good one ($R^2 = 0.997$), was obtained for the logarithmic function. This behavior is the signature of weak localization in 2D [47]. The coefficient of $\ln(T)$ seems to support this possibility: $\Delta\sigma_{square} = c\Delta\rho/\rho^2 \approx 8 \times 10^{-5}\ln(T)$ Ω^{-1}, where c (= 3.53 Å) is the lattice parameter

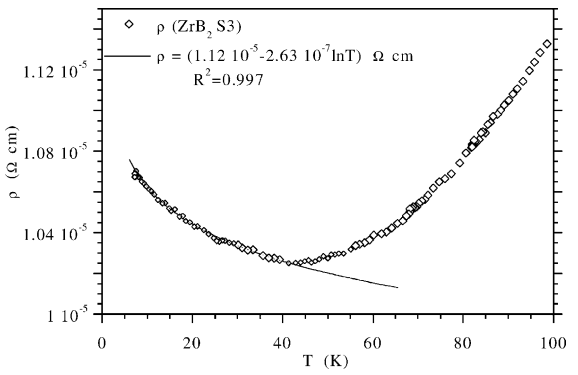

Fig. 3. The shallow minimum in ρ versus T for sample ZrB_2 S3 at low temperatures. The solid line represents the fitted logarithmic function that indicates weak localization (see text).

of ZrB_2; the coefficient of $\ln(T)$ in $\Delta\sigma_{square}$ is very close to the value of $G_0 = 2e^2/h$ ($= 7.75 \times 10^{-5}$ Ω^{-1}), of the order of the theoretical coefficient. The origin of the weak disorder in S2 and S3 may be carbon impurities from the graphite crucible or deviations from stoichiometry. As shown below, the thermopower of the ZrB_2 samples S2 and S3 provides further support for weak localization. The shallow minimum discussed above had a negligible effect on the fitting parameters of the BG formula. It can be seen that θ_R varies little from sample to sample; it is much larger than that found in Ref. [41] but closer to θ_D (see Table 1).

A narrow step was observed around 5.4 K in the AC magnetic susceptibility of sample S1; it was about 0.3% of the step found (around 87 K) for an YBCO sample of comparable volume. A similar step was observed around 3 K for the unprocessed commercial powder. AC susceptibility showed no marks of a transition to superconductivity in S2 and S3 and in the powder synthesized by us.

3.2. Temperature dependence of thermopower

Fig. 4 represents $S(T)$ for MgB_2, AlB_2 and ZrB_2 samples on which $\rho(T)$ was measured. The most prominent feature of this figure is that $S(T)$ for MgB_2 and ZrB_2 lie on both sides of $S = 0$ almost as *mirror images* of one another with $S(T)$ of AlB_2 lying in the middle, with almost zero values for all temperatures.

Looking for systematics in $S(T)$ for these materials was rewarding. The details, specific for each system, will be discussed prior to drawing conclusions on the systematics.

In general there is good agreement between $S(T)$ of the MgB_2 HP sample and most of the earlier results in the overlapping ranges of temperature. The solid line through the low-T data points represents $S = -1 + 0.034T$ μV/K. In Refs. [4,11,13–15] the RT values of S range between 7 and 8.7 μV/K, those of dS/dT in the linear regime range between 0.035 and 0.042 μV/K^2. There is also agreement on the negative extrapolated value of S at $T = 0$. The $S(T)$ data for the NA MgB_2 sample are very close to those of the HP sample in the regime where $S(T)$ is linear; this, in spite of the

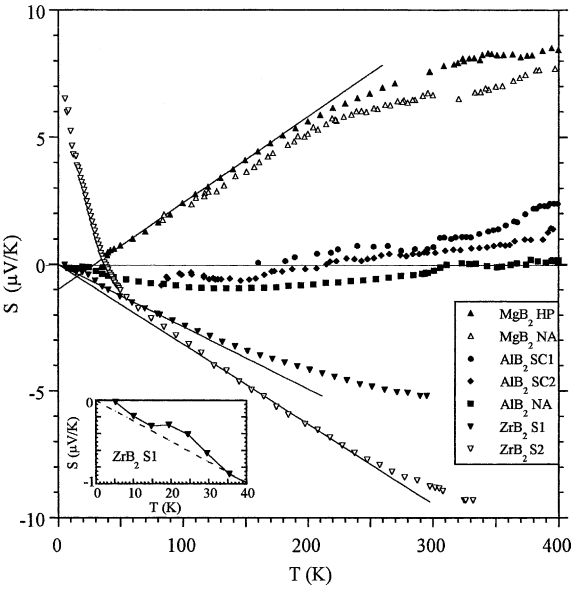

Fig. 4. S versus T for samples of MgB_2, AlB_2 and ZrB_2 on which resistivity was measured (see Fig. 1 and Table 1). The solid line that passes through data points for the MgB_2 HP sample represents $S = -1 + 0.034T$ μV/K and the two solid lines that pass through data points for ZrB_2 S1 and S2 represent $S = -0.025T$ and $S = -0.032T$ μV/K, respectively. Low temperature $S(T)$ for ZrB_2 S1 is shown on an expanded scale in the inset. The low temperature range of $S(T)$ for S2 is replotted in Fig. 5.

fact that the residual resistivities of these two samples are different by more than two orders of magnitude. This emphasizes the weak sensitivity of the thermopower to grain-boundaries and porosity. The difference between $S(T)$ for the HP and NA samples is larger at high temperatures where $S(T)$ is non-linear and tends to saturate.

Up to RT, $S(T)$ for the AlB_2, NA and SC samples, lie within ±1 μV/K. Above RT, S for the polycrystal remains zero and that of the SCs increases up to 1.5 and 2.5 μV/K. As in the case of MgB_2, the microstructure (or composition) affects $S(AlB_2)$ mainly at high temperatures. It is notable that at high temperature, the sign of S for the AlB_2 SC samples (+) is the same as that of the RT Hall constant [30]. $N(E)$ in the pseudogap is probably non-symmetric. With increasing temperature the increasing ΔE window around E_F may contain more hole-like than electron-like states leading to positive S and R_H.

$S(T)$ for the ZrB_2 S1 (sintered at 1500 °C) and S2 (sintered at 1800 °C) are quasilinear over wide ranges of temperature. The straight lines that pass through the data points in this region represent $S = -0.025T$ μV/K and $S = -0.032T$ μV/K, for S1 and S2, respectively. The reproducibility of $S(T)$ for samples prepared differently is poorer than for MgB_2. Above ~150 K for S1 and ~250 K for S2, the corresponding $S(T)$ become nonlinear exhibiting a tendency towards saturation, very similar to that of $S(MgB_2)$. $S(T)$ of S1 at low temperatures is shown on an expanded scale in the inset of Fig. 4. A minute but reproducible deviation from the straight line is observed around 20 K; it resembles what one would expect for phonon drag thermopower in a dirty metal. At 5 K $S \approx -0.01$ μV/K, i.e. zero within the experimental uncertainty as expected for a superconductor. However, a thin, percolating superconducting filament could account for this result.

Below ~50 K, $S(T)$ for ZrB_2 S2 deviates from the straight line, crosses the $S = 0$ line at $T = 38$ K and increases steeply with further decrease of T. This behavior was exhibited by several samples sintered at 1800 °C and accompanies their $\rho(T)$ bearing the signature of weak localization. There have been conflicting predictions for the thermopower in the weak-localization regime; recent results suggest a $\ln(1/T)$ dependence of S [49]. $S(T)$ for samples S2 and S3 below 40 K is plotted as function of temperature on a linear-log scale in Fig. 5. At least for S3 the logarithmic function fits remarkably well the experimental plot ($R^2 = 0.998$). The inset of Fig. 5 shows $\rho(T)$ for S3 (shown before in Fig. 3), replotted on a linear-log scale. To our knowledge this is a rare example of evidence for weak localization in 2D, based on both $\rho(T)$ and $S(T)$ dependencies.

We now return to the gross features of $S(T)$ and show that these seem to be correlated with $dN(E)/dE|_{E_F}$. Inspection of the available $N(E)$ graphs shows that $dN(E)/dE|_{E_F}$ is negative for MgB_2 [16,32,40,50], positive for ZrB_2 [35,38–40] and ~0 for AlB_2 [31–33]. For spherical equi-energy surfaces and elastic scattering this correlation is straightforward since $\sigma(E) \propto v^2(E)\tau(E)N(E)$ where $v(E)$ is the energy dependent velocity, and the derivative of $v^2(E)\tau(E)$ has the same sign as that of

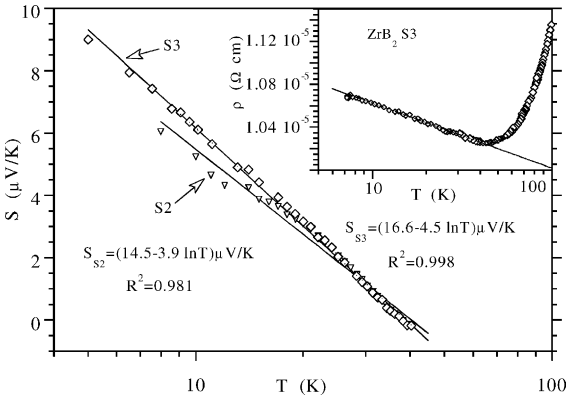

Fig. 5. S versus T for the nonsuperconducting ZrB_2 S2 and S3 samples plotted on a linear-log scale. ρ versus T for sample ZrB_2 S3 plotted on linear-log scale is shown in the inset.

$N(E)$ [9]. Suppose that this relation, with $N(E)$ and the diffusivity D ($\propto v^2(E)\tau(E)$) replaced by averages over equi-energy surfaces may be extended to our systems. The question "which of the two terms $d\ln N(E)/dE|_{E_F}$ and $d\ln D(E)/dE|_{E_F}$ dominates $d\ln\sigma(E)/dE|_{E_F}$" might be posed. The answer ($d\ln N(E)/dE|_{E_F}$) is simple in the case of AlB_2 for which $dN/dE|_{E_F} \approx 0$ and $S \approx 0$. The values of dS/dT for MgB_2 HP and ZrB_2 S1 and S2 yield: $d\ln\sigma(E)/dE_{E_F} \approx -1.4$, $+1.0$ and $+1.3$ eV^{-1}, respectively. Within the limited resolution of the available $N(E)$ graphs around E_F we checked if $(1/N)dN/dE|_{E_F}$ can reach -1.4 and $+1.3$ eV^{-1}, for MgB_2 and ZrB_2, respectively. In Fig. 2 of Ref. [16] $N(E)$ of MgB_2 has a steep *negative* slope around E_F where $N(E) \sim 0.7$; inspection of that graph shows that dN/dE could be -1 eV^{-2}. In Fig. 3 of Ref. [38] $N(E)$ of ZrB_2 has a steep positive slope around E_F where $N(E) \sim 0.3$; according to this figure dN/dE_{E_F} could be $+0.4$ eV^{-2}; however, dN/dE_{E_F} in Fig. 1 of Ref. [39] seems larger. In spite of this uncertainty it seems that $(1/N)dN/dE|_{E_F}$ plays an important role in $S(T)$ of all three materials.

4. Summary and final remarks

Resistivity and thermopower measurements were carried out on polycrystalline samples of the

three title materials and on SCs of AlB_2. The polycrystalline samples were either hot-pressed (MgB_2 HP), sintered at various temperatures (ZrB_2 S1–S3) or just compacted at RT (MgB_2 NA and AlB_2 NA). Single crystal growth was attempted for all three materials but only the AlB_2 crystals were large enough for both resistivity and thermopower measurements.

For all samples $\rho(T)$ exhibited BG-like temperature dependencies. Fitting the textbook formula to the $\rho(T)$ graphs for MgB_2 and ZrB_2 gave characteristic temperatures (θ_R) that vary little from sample to sample and fall close to the respective Debye temperatures obtained from thermal measurements. Larger θ_R values are obtained from fitting to the experimental plots a generalized BG function (BG(3)). A widespread of θ_R values was obtained for the AlB_2 samples. Using the case of AlB_2 NA sample having the largest ρ_0 and lowest fitted θ_R, it was shown that the widespread of θ_R values among the AlB_2 samples may be due to competition between phonon scattering and scattering from vibrating impurities [46].

MgB_2 samples with resistivities different by more than two orders of magnitude exhibited superconductivity below only slightly different transition temperatures. Marks of low-T superconductivity (at $\sim$5.5 K) were obtained in the AC susceptibility and thermopower measurements in a sample of ZrB_2 processed at low temperatures. These marks may be due to a foreign phase, as proposed for previously published results [42]. No marks of superconductivity were detected in samples of ZrB_2 processed at higher temperatures, having much lower resitivities. At low temperatures the resistivity and thermopower of these samples exhibit a logarithmic dependence on temperature, typical for weak localization in 2D.

At high temperatures the thermopower $S(T)$ for ZrB_2 (n-type) is almost the mirror image of $S(T)$ for MgB_2 (p-type) while $S(AlB_2)$ is very small at all temperatures. Using available graphs of the DOS distribution $N(E)$ around E_F, it is shown that for MgB_2 and ZrB_2 the sign of S is that of $-\mathrm{d}\ln N(E)/\mathrm{d}E$. Rough estimates of $\mathrm{d}\ln N(E)/\mathrm{d}E|_{E_F}$ are consistent with the possibility that this term represents the main contribution to the magnitude of S. Thus, it may not be accidental that for AlB_2 $\mathrm{d}N(E)/\mathrm{d}E|_{E_F} \sim 0$ and $S(E)$ is very small at all temperatures.

The results of this work suggest that measuring transport properties of additional diborides may be rewarding. The first choices would be materials for which calculated and/or experimental $N(E)$ around E_F results are available. It would also be interesting to investigate diborides for which there are conflicting reports about superconductivity.

Acknowledgements

We are grateful to Mrs. G. Bazalitsky for programming the curve fitting of the BG and RS functions. Helpful discussions with V.A. Gasparov are gratefully acknowledged. This research was supported by the Center of Absorption in Science, Ministry of Immigrant Absorption, by the Posnansky Research Fund for HTSC, and by the JCG Research Fund.

References

[1] J. Nagamatsu, N. Nakagawa, T. Muranaka, Y. Zenitani, J. Akimitsu, Nature 410 (2001) 63.
[2] X.H. Chen, Y.S. Wang, Y.Y. Xue, R.L. Meng, Y.Q. Wang, C.W. Chu, Phys. Rev. B 65 (2002) 024502.
[3] A.V. Sologubenko, J. Jun, S.M. Kazakov, J. Karpinski, H.R. Ott, cond-mat/0111273, 2001;
Phys. Rev. B 66 (2002) 014504.
[4] M. Putti, E. Galleani d'Agliano, D. Marré, F. Napoli, M. Tassisto, P. Manfrinetti, A. Palenzona, C. Rizzuto, S. Massidda, Eur. Phys. J. B 25 (2002) 439.
[5] K.H.P. Kim, J.H. Choi, C.U. Jung, P. Chowdhury, H.S. Lee, M.S. Park, H.J. Kim, J.Y. Kim, Z. Du, E.M. Choi, M.S. Kim, W.N. Kang, S.I. Lee, G.Y. Sung, J.Y. Lee, Phys. Rev. B 65 (2002) 100510.
[6] Y. Eltsev, S. Lee, K. Nakao, N. Chikumoto, S. Tajima, N. Koshizuka, M. Murakami, Phys. Rev. B 65 (2002) 140501.
[7] A.K. Pradhan, M. Tokunaga, Z.X. Shi, Y. Tagano, H. Kito, H. Ihara, T. Tamegai, Phys. Rev. B 65 (2002) 144513.
[8] J.M. Ziman, Electrons and Phonons, Clarendon Press, Oxford, 1960.
[9] F.J. Blatt, Physics of electronic conduction in metals, McGraw-Hill Book Company, New York, 1968.
[10] A.H. Wilson, Proc. R. Soc. London, Ser. A 167 (1938) 580.
[11] B. Lorenz, R.L. Meng, Y.Y. Xue, C.W. Chu, Phys. Rev. B 64 (2001) 052513;
B. Lorenz, Y.Y. Xue, R.L. Meng, C.W. Chu, cond-mat/0110125, 2001.

[12] T. Muranaka, J. Akimitsu, M. Sera, Phys. Rev. B 64 (2001) 020505.
[13] W. Liu, J. Huang, Y. Wang, X. Wang, Q. Feng, S. Yan, Solid State Commun. 118 (2001) 575.
[14] E.S. Choi, W. Kang, J.Y. Kim, M.S. Park, C.U. Jung, H.J. Kim, S.I. Lee, cond-mat/0104454, 2001.
[15] M. Schneider, D. Lipp, A. Gladun, P. Zahn, A. Handstein, G. Fuchs, S.-L. Drechsler, M. Richter, K.-H. Müller, H. Rosner, Physica C 363 (2001) 6.
[16] J. Kortus, I.I. Mazin, K.D. Belashchenko, V.P. Andropov, L.L. Boyer, Phys. Rev. Lett. 86 (2001) 4656.
[17] J.M. An, W.E. Pickett, Phys. Rev. Lett. 86 (2001) 4366.
[18] A.Y. Liu, I.I. Mazin, J. Kortus, Phys. Rev. Lett. 87 (2001) 87005;
I.I. Mazin, J. Kortus, Phys. Rev. B 65 (2002) 180510.
[19] H. Uchiyama, K.M. Shen, S. Lee, A. Damascelli, D.H. Lu, D.L. Feng, Z.-X. Shen, S. Tajima, Phys. Rev. Lett. 88 (2002) 157002.
[20] J.J. Tu, G.L. Carr, V. Perebeinos, C.C. Homes, M. Strongin, P.B. Allen, W.N. Kang, E.-M. Choi, H.-J. Kim, S.-I. Lee, Phys. Rev. Lett. 87 (2001) 277001.
[21] F. Marsiglio, Phys. Rev. Lett. 87 (2001) 247001.
[22] E. Cappelluti, S. Ciuchi, C. Grimaldi, L. Pietronero, S. Strässler, Phys. Rev. Lett. 88 (2002) 117003.
[23] M. Jonson, G.D. Mahan, Phys. Rev. B 42 (1990) 9350, and references therein.
[24] K. Durczewski, M. Ausloos, Phys. Rev. B 61 (2000) 5303, and references therein.
[25] J. Castaing, P. Costa, Properties and uses of diborides, in: Boron and Refractory Borides, Springer-Verlag, Berlin, West Germany, 1977.
[26] D.J. Bergman, D. Stroud, in: Ehrenreich, Turnbull (Eds.), Solid State Physics, vol. 47, Academic Press, San-Diego, 1992, p. 147, and references therein.
[27] For a review see C. Buzea, T. Yamashita, Supercond. Sci. Technol. 14 (2001) R115.
[28] R.K. Williams, R.S. Graves, F.J. Weaver, J. Appl. Phys. 59 (1986) 1552.
[29] G.E. Grechnev, N.V. Ushakova, P.V. Kervalishvili, G.G. Kvachantiradze, K.S. Kharebov, Low Temp. Phys. 23 (1997) 217.
[30] E. Sirtl, L.M. Woerner, J. Cryst. Growth 16 (1972) 215.
[31] K. Lie, R. Høier, R. Brydson, Phys. Rev. B 61 (2000) 1786.
[32] J. Nakamura, N. Yamada, K. Kuroki, T.A. Callcott, D.L. Ederer, J.D. Denlinger, R.C.C. Perera, Phys. Rev. B 64 (2001) 174504.
[33] J. Nakamura, M. Watanabe, T. Oguchi, S. Nasubida, E. Kabasawa, N. Yamada, K. Kuroki, H. Yamazaki, S. Shin, Y. Umeda, S. Minakawa, N. Kimura, H. Aoki, J. Phys. Soc. Jpn. 71 (2002) 408.
[34] J.S. Slusky, N. Rogado, K.A. Regan, M.A. Hayward, P. Khalifah, T. He, K. Inumaru, S.M. Loureiro, M.K. Haas, H.W. Zandbergen, R.J. Cava, Nature 410 (2001) 343.
[35] D.L. Johnson, B.N. Harmon, S.H. Liu, J. Chem. Phys. 73 (1980) 1898.
[36] J. Piper, J. Phys. Chem. Solids 27 (1966) 1907.
[37] H. Ihara, M. Hirabayashi, H. Nakagawa, Phys. Rev. B 16 (1977) 726.
[38] P. Vajeeston, P. Ravindran, C. Ravi, R. Asokamani, Phys. Rev. B 63 (2001) 045115.
[39] H. Rosner, J.M. An, W.E. Pickett, S.-L. Drechsler, cond-mat/203030, 2002;
Phys. Rev. B 66 (2002) 024521.
[40] I.R. Shein, A.L. Ivanovskii, cond-mat/0109445, 2001.
[41] V.A. Gasparov, N.S. Sidorov, I.I. Zve'rkova, M.P. Kulakov, JETP Lett. 73 (2001) 532.
[42] V.A. Gasparov, private communication.
[43] I. Higashi, Y. Takahashi, T. Atoda, J. Cryst. Growth 33 (1976) 207.
[44] S. Muranaka, S. Kawai, J. Cryst. Growth 26 (1974) 165.
[45] C. Deppisch, G. Liu, A. Hall, Y. Xu, A. Zangvil, J.K. Shang, J. Economy, J. Mater. Res. 13 (1998) 3485.
[46] M.Yu. Reizer, A.V. Sergeev, Zh. Eksp. Theor. Fiz. 92 (1987) 2291 (Sov. Phys. JETP 65 (1987) 1291);
P.M. Echternach, M.E. Gershenson, H.M. Bozler, Phys. Rev. B 47 (1993) 13659;
N.G. Ptitsina, G.M. Chulkova, K.S. Il'in, A.V. Sergeev, F.S. Pochinkov, E.M. Gershenzon, M.E. Gershenson, Phys. Rev. B 56 (1997) 10089;
K.S. Il'in, N.G. Ptitsina, A.V. Sergeev, G.N. Gol'tsman, E.M. Gershenzon, B.S. Karasik, E.V. Pechen, S.I. Krasnosvobodtsev, Phys. Rev. B 57 (1998) 15623.
[47] P.A. Lee, T.V. Ramakrishnan, Rev. Mod. Phys. 57 (1985) 287.
[48] P. Ravindran, P. Vajeeston, R. Vidya, A. Kjekshus, H. Fjellvåg, Phys. Rev. B 64 (2001) 224509, Table 3.
[49] R.C. Budhani, M.C. Sullivan, C.J. Lobb, R.L. Greene, Phys. Rev. B 65 (2002) 100517, and references therein.
[50] E.Z. Kurmaev, I.I. Lyakhovskaya, J. Kortus, A. Moewes, N. Miyata, M. Demeter, N. Neumann, M. Yanagihara, M. Watanabe, T. Muranaka, J. Akimitsu, Phys. Rev. B 65 (2002) 134509.